



Luminescence and Energy Transfer Studies of $\text{Sr}_3\text{Al}_2\text{O}_6:\text{Ce}^{3+}, \text{Tb}^{3+}$ and $\text{Sr}_3\text{Al}_2\text{O}_6:\text{Tb}^{3+}, \text{Eu}^{3+}$ Phosphors

Pallavi Page* and K.V.R. Murthy

Display Materials Laboratory, Applied Physics Department, Faculty of Technology and Engineering,
The M. S. University of Baroda, Vadodara, India

Abstract— We report here energy transfer phenomenon occurred in single-phased $\text{Sr}_3\text{Al}_2\text{O}_6:\text{Ce}^{3+}, \text{Tb}^{3+}$ and $\text{Sr}_3\text{Al}_2\text{O}_6:\text{Tb}^{3+}, \text{Eu}^{3+}$ phosphors for the application in fluorescent lamps. The energy transfer phenomenon in $\text{Sr}_3\text{Al}_2\text{O}_6:\text{Ce}^{3+}, \text{Tb}^{3+}$ and $\text{Sr}_3\text{Al}_2\text{O}_6:\text{Tb}^{3+}, \text{Eu}^{3+}$ systems were observed as a result of increasing concentration of cerium and europium in $\text{Sr}_3\text{Al}_2\text{O}_6:\text{Tb}^{3+}$ system. The $\text{Sr}_3\text{Al}_2\text{O}_6:\text{Ce}^{3+}, \text{Tb}^{3+}$ phosphor exhibits emission over blue and green region of the visible spectrum corresponding to $^5\text{D}_3-^7\text{F}_J$ transitions and $^5\text{D}_4-^7\text{F}_J$ transitions of Tb^{3+} ions. The addition of Ce^{3+} in the $\text{Sr}_3\text{Al}_2\text{O}_6:\text{Tb}^{3+}$ results in enhancing the 5D_3 transitions of Tb^{3+} . Whereas $\text{Sr}_3\text{Al}_2\text{O}_6:\text{Tb}^{3+}, \text{Eu}^{3+}$ phosphor when excited by 254 nm shows sharp lines peaked in 400–550 nm due to $^5\text{D}_3-^7\text{F}_J$ transitions and $^5\text{D}_4-^7\text{F}_J$ transitions of Tb^{3+} ions and sharp peaks in the orange–red region (580–700 nm) originating from $^5\text{D}_0-^7\text{F}_J$ transitions of Eu^{3+} ions. The thermoluminescence study was performed on the β -irradiated c to study its change in trap depths due to addition of cerium and europium as co-activator. Thus from the above studies it is observed that $\text{Sr}_3\text{Al}_2\text{O}_6:\text{Ce}^{3+}, \text{Tb}^{3+}$ phosphors are good contestant for bluish green and yellowish white light emitting phosphors.

1. INTRODUCTION

Rare earth based research has been the backbone of the display industry and still the $4f_n$ levels play significant role in enhancing and improving the industry with their charming and fascinating spectroscopic transitions. Although the commercial FLs contains a mixture of triphosphors—the blue-emitting $\text{BaMgAl}_{10}\text{O}_{17}:\text{Eu}^{2+}$ [1], the red-emitting $\text{Y}_2\text{O}_3:\text{Eu}^{3+}$ [2], and the green-emitting $\text{LaPO}_4:\text{Ce}^{3+}, \text{Tb}^{3+}$ [3] under UV light at 254 nm were well-established, the development of new phosphors continues because of the importance of phosphor efficiency required for different applications [4,5]. As we known, trivalent Ce, Tb and Eu ions, as the promising species that provide optical emission in blue, green and red regions, have been investigated by many groups [6,7].

The process of transferring the excitation energy from donor to acceptor is called energy transfer. The center, which absorbs and transfers energy, is called the sensitizer and the center to which the absorbed energy transferred to is called activator. Energy transfer can occur between two identical luminescent centers or between two non-identical centers. According to the theory of energy transfer developed by Förster (1948) and later by Dexter (1953) the efficiency of energy transfer [8] depends mainly on the extent of spectral overlap between the absorption band of acceptor and emission band of donor with the suitable interaction between them [9].

The addition of the co-dopant in the $\text{Sr}_3\text{Al}_2\text{O}_6:\text{Eu}^{2+}$ system is also studied and has a useful application as a mechanoluminescent phosphor [10]. The $\text{SrAl}_2\text{O}_4:\text{Eu}^{2+}, \text{Dy}^{3+}$ is famous for its long light persistence property is one such material that has been studied extensively for more than a decade now [11, 12]. In our earlier work, we have reported the photoluminescence and thermoluminescence properties of rare earth doped $\text{Sr}_3\text{Al}_2\text{O}_6$ phosphor [13, 14, 15]. In this paper we study the effect of addition of Ce and Eu^{3+} in the $\text{Sr}_3\text{Al}_2\text{O}_6:\text{Tb}^{3+}$ phosphor on its optical and thermoluminescent properties. To study the effect of the beta irradiation on the nature and type of traps and to understand the mechanism by which the radiative recombination is taking place, the thermoluminescence glow curves were recorded. The energy transfer phenomenon was also studied by keeping the concentration of Tb^{3+} constant and varying the concentration of Ce^{3+} and Eu^{3+} in the system. The effect of incorporation of co-activator in the $\text{Sr}_3\text{Al}_2\text{O}_6:\text{Tb}^{3+}$ system was also reported in the case of thermoluminescence study.

2. EXPERIMENTAL

2.1 Sample Preparation

The synthesis of the $\text{Sr}_3\text{Al}_2\text{O}_6$ doped with rare earths has been elaborated in our previous papers [13,14]. The phosphor samples were prepared by the sol-gel reflux technique. The starting materials taken were strontium nitrate, aluminum nitrate and the rare earths in the nitrate form. All of them were acquired from S.D. Fine Chemicals with rare earths of purity 99.9%. The first set of the samples was prepared by doping the Terbium nitrate (1%) and Europium nitrate (x%) in the host matrix.

* Corresponding Author Email: pallavipage@gmail.com

The powders were weighed according to the nominal composition of $\text{Sr}(\text{NO}_3)_2 + \text{Al}(\text{NO}_3)_3 \cdot 9\text{H}_2\text{O} + \text{Tb}(\text{NO}_3)_3 + x \text{Eu}(\text{NO}_3)_3$ ($x = 0.025\%, 0.1\%, 0.5\%$). Second set of samples were prepared by doping the Terbium nitrate (0.025%) and Cerium nitrate ($x\%$) in the host matrix. The powders were weighed according to the nominal composition of $\text{Sr}(\text{NO}_3)_2 + \text{Al}(\text{NO}_3)_3 \cdot 9\text{H}_2\text{O} + \text{Tb}(\text{NO}_3)_3 + x \text{Ce}(\text{NO}_3)_3$ ($x = 0.05\%, 0.1\%$).

The starting materials strontium and aluminum nitrates were taken in 1:2 proportions and dissolved in the appropriate amount of distilled water and kept for stirring. Thereafter the rare earths compounds with different concentrations were mixed to the above solution. Citric acid and ethylene glycol were added to the solution after one hour of constant stirring. The resulting gel was set for refluxing at 100°C for 3 hours. The gel thus obtained, was kept for drying in an oven maintained at 100°C for 10 hours. The yellowish gel then transformed into fluffy material. It was then kept for firing at a temperature maintained at 900°C in a furnace for 16 hours in air. The white powder obtained on firing, was ground using an agate mortar and pestle and was then subjected to various characterizations.

2.2 X-Ray Diffraction, Photoluminescence and Thermoluminescence Characterization

Phase identification of the powders was carried out by the X-ray powder diffraction using RIGAKU D'MAX III Diffractometer having $\text{Cu K}\alpha$ radiation. The photoluminescence (Emission and Excitation spectra) were recorded at room temperature using spectrofluorophotometer RF-5301 of SHIMADZU make with a xenon source. The slit width of both the excitation and the emission monochromator was kept at 1.5nm and the sensitivity was kept high for all the samples. The thermoluminescence glow curve of all the samples were recorded using Nucleonix-1009 make thermoluminescence reader at a constant heating rate of 2.0°C/s . The amount of sample used for studying TL was 5mg and was irradiated with β rays from a Sr-90 source of 50 mCi strength.

3. RESULT AND DISCUSSION

3.1 X-Ray Diffraction Studies

In order to determine the crystal structure and phase purity of the phosphors, X-ray diffraction (XRD) analysis was carried out. Figure – 1 shows X-ray diffraction (XRD) pattern of the $\text{Sr}_3\text{Al}_2\text{O}_6\text{:Tb}^{3+}(1\%), \text{Eu}^{3+}(0.1\%)$ phosphor. From the XRD pattern analysis it was found that the prominent phase formed was $\text{Sr}_3\text{Al}_2\text{O}_6$. The $\text{Sr}_3\text{Al}_2\text{O}_6$ phase belongs to the space group $\text{pa}3$ having a cubic crystalline structure [16]. The traces of other phases of $\text{SrO-Al}_2\text{O}_3$ system were very weak. As the XRD patterns are similar for all the terbium and europium concentrations as well as for cerium and terbium concentrations, only one with 1% Tb^{3+} and 0.1% Eu^{3+} has

been shown and it matches very well with that reported by Kennedy et al. [17].

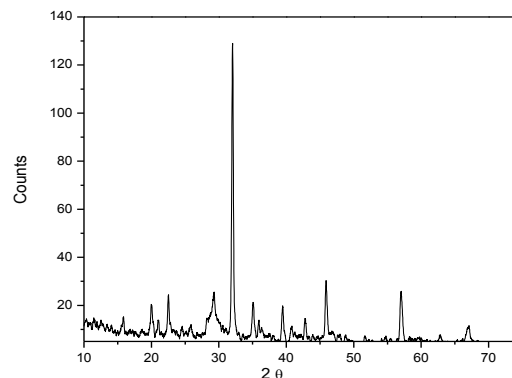


Fig. 1: XRD pattern of $\text{Sr}_3\text{Al}_2\text{O}_6\text{:Tb}^{3+}(1\%), \text{Eu}^{3+}(0.1\%)$

3.2 Photoluminescence of $\text{Sr}_3\text{Al}_2\text{O}_6\text{:Tb}^{3+}, \text{Eu}^{3+}$ Phosphor

Figure 2 shows the excitation and emission spectra of the $\text{Sr}_3\text{Al}_2\text{O}_6\text{:Tb}^{3+}, \text{Eu}^{3+}$ system when excited with the 254nm

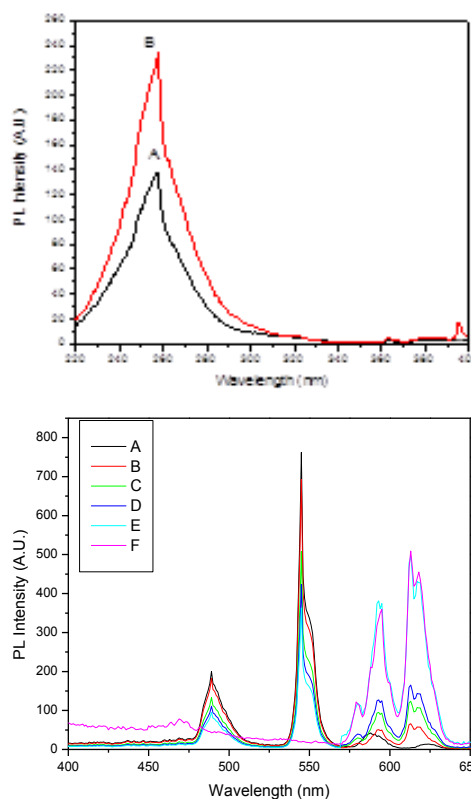


Fig. 2: Excitation and Emission characteristics of $\text{Sr}_3\text{Al}_2\text{O}_6\text{:Tb}^{3+}(1\%), \text{Eu}^{3+}(x\%)$.
For emission the excitation wavelength = 254 nm
Curve A = $\text{Sr}_3\text{Al}_2\text{O}_6\text{:Tb}(1\%)$;
B = $\text{Sr}_3\text{Al}_2\text{O}_6\text{:Tb}(1\%), \text{Eu}(0.025\%)$;
C = $\text{Sr}_3\text{Al}_2\text{O}_6\text{:Tb}(1\%), \text{Eu}(0.1\%)$;
D = $\text{Sr}_3\text{Al}_2\text{O}_6\text{:Tb}(1\%), \text{Eu}(0.5\%)$;
E = $\text{Sr}_3\text{Al}_2\text{O}_6\text{:Tb}(1\%), \text{Eu}(1\%)$;
F = $\text{Sr}_3\text{Al}_2\text{O}_6\text{:Eu}(1\%)$

wavelength. The excitation spectra were measured for 545 nm of Tb^{3+} (1%) emission. All the samples show excitation nearly same except increase in the intensity of the 390nm peak of Eu^{3+} transition on increasing the Eu^{3+} concentration. Hence only two excitation spectra are represented in the figure. The curve A shows the emission pattern of Tb^{3+} (1%) having narrow band emission at 489, 545, 585 and 625 nm for the characteristic multiplet transition of $^5D_4 \rightarrow ^7F_{J=6,5,4,3}$ respectively [18].

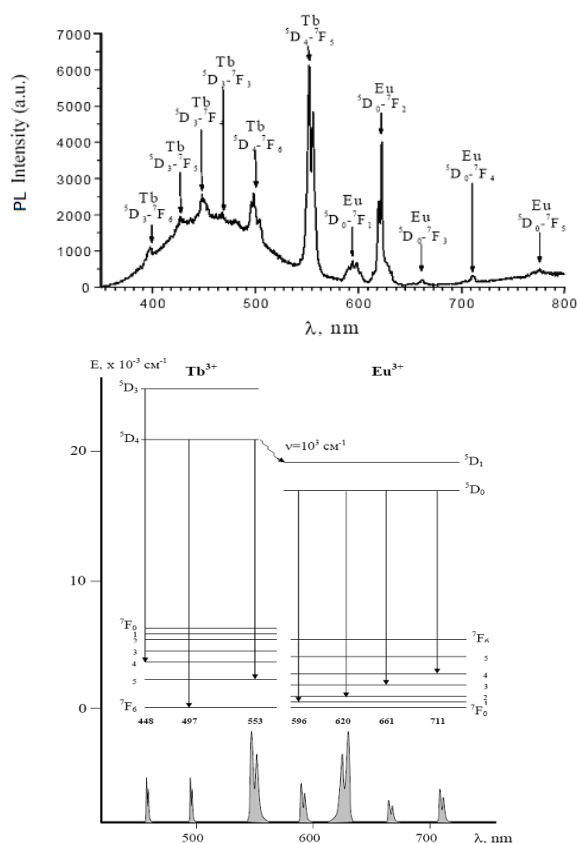


Fig. 3: Expected PL spectra and Schematic representation of the energy transfer in $Sr_3Al_2O_6: Tb^{3+}, Eu^{3+}$

In particular, the highest sharp line peaked at 542nm is characteristic of $^5D_4 \rightarrow ^7F_5$ of Tb^{3+} 4f-4f transitions. Curve B shows the emission spectra of $Sr_3Al_2O_6: Tb(1\%), Eu(0.025\%)$. The intensity of the terbium emission band decreases slightly and the characteristic emission of trivalent Eu is observed at 580 nm, 592 nm, 595 nm, 613 nm, 617 nm ascribed to $^5D_0 \rightarrow ^7F_J$ ($J = 0, 1, 2$) multiplet transitions [19]. Hence this indicates the possibility of energy transfer occurs between Tb^{3+} and Eu^{3+} ions in the host lattice. To observe further the energy transfer phenomenon, we slowly increased the concentration of the Eu^{3+} in the system by keeping the concentration of terbium constant i.e. 1%. The concentration of europium was increased from 0.025% to 1%. The emission spectra of this double doped system signifies that the emission intensity of terbium decreases nonlinearly and Eu^{3+} increases linearly with increase in europium concentration. The emission spectra of $Sr_3Al_2O_6: Tb^{3+}$

(1%), Eu^{3+} (1%) i.e., curve E shows a beautiful yellowish white emission can be obtained from this phosphor when excited with the ultraviolet wavelength (254 nm). The corresponding energy levels scheme of Tb^{3+} and Eu^{3+} and the possible optical transition involved in the energy transfer processes are schematically depicted in Fig. 3. Out of all these emissions we observed only emissions shown in Figure 2. The 5D_3 transition of Tb^{3+} is already absent due to the cross relaxation at higher concentration and the Eu^{3+} shows only the transition $^5D_0 \rightarrow ^7F_J$ ($J = 0, 1, 2$). When Tb^{3+} ions absorb UV light, the excitation energy could be released not only by emitting green light but also by transferring some of its emission energy to Eu^{3+} ions, which finally exhibits a yellowish white emission of Tb^{3+} and Eu^{3+} ions.

3.3 Photoluminescence of $Sr_3Al_2O_6: Tb^{3+}, Ce^{3+}$ Phosphor

Figure 4 shows the excitation and emission spectra of the $Sr_3Al_2O_6: Tb^{3+}$ sample co-doped with Ce^{3+} . The doping concentration of the Tb^{3+} in the phosphor samples was kept as 0.025 mol% for the studies and the concentration of Ce^{3+} was kept as 0.05mol% and 0.1mol%, respectively. The excitation spectra were obtained by monitoring emissions peaks for Tb^{3+} i.e., 545nm. The excitation curve of $Sr_3Al_2O_6: Tb^{3+}$ (0.025%), Ce^{3+} (0.1%) and $Sr_3Al_2O_6: Tb^{3+}$ (0.025%), Ce^{3+} (0.05%) show the peaks around 254nm and 240nm. The excitation spectra of

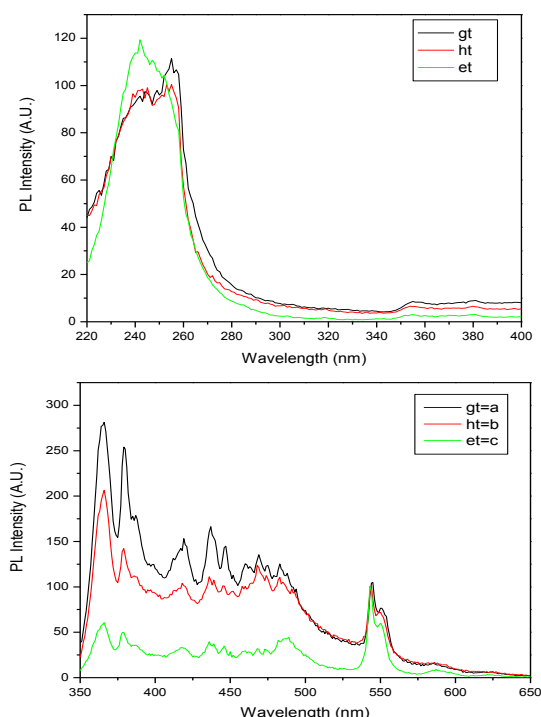


Fig. 4: PL excitation spectra of $Sr_3Al_2O_6: Tb, Ce$. Emission: 545 nm.

**Curve gt = $Sr_3Al_2O_6: Tb(0.025\%), Ce(0.1\%)$;
ht = $Sr_3Al_2O_6: Tb(0.025\%), Ce(0.05\%)$;
et = $Sr_3Al_2O_6: Tb(0.025\%)$**

$\text{Sr}_3\text{Al}_2\text{O}_6:\text{Tb}^{3+}$ (0.025%) shows peak around 254 nm which corresponds to the charge transfer transition of Tb^{3+} . The new band at around 240nm is formed due to incorporation of Ce^{3+} in the phosphor. The excitation spectrum of the double-doped phosphors seems to contain a significant additional contribution from the Ce^{3+} absorption. Ce^{3+} can strongly absorb UV radiation and efficiently transfer its energy to Tb^{3+} . This process of energy transfer from Ce^{3+} donor to Tb^{3+} acceptor has been observed in many phosphors such as $\text{CaAl}_4\text{O}_7:\text{Tb}^{3+}, \text{Ce}^{3+}$ and for Ce^{3+} in other hosts [20-22].

The emission spectra of $\text{Sr}_3\text{Al}_2\text{O}_6:\text{Tb}^{3+}$ (0.025%), $\text{Sr}_3\text{Al}_2\text{O}_6:\text{Tb}^{3+}$ (0.025%), Ce^{3+} (0.1%) and $\text{Sr}_3\text{Al}_2\text{O}_6:\text{Tb}^{3+}$ (0.025%), Ce^{3+} (0.05%) are as shown in figure4 when excited with 254 nm wavelength. The curve of $\text{Sr}_3\text{Al}_2\text{O}_6:\text{Tb}^{3+}$ (0.025%), Ce^{3+} (0.1%) and $\text{Sr}_3\text{Al}_2\text{O}_6:\text{Tb}^{3+}$ (0.025%), Ce^{3+} (0.05%) shows the luminescence from $^5\text{D}_3$ level of Tb^{3+} along with the $^5\text{D}_4$ transitions. Addition of Ce^{3+} into the $\text{Sr}_3\text{Al}_2\text{O}_6:\text{Tb}^{3+}$ system increases the intensity of the $^5\text{D}_3$ transitions than that of the $^5\text{D}_4$ levels. The system shows transitions observed at 365, 379, 418, 437, 447, 460, 470, 475, 482, 545 nm. The emission peaks observed above 400 nm are prescribed to $^5\text{D}_3$ to $^7\text{F}_j$ ($j = 5, 4, 3, 2, 1, 0$) transitions. Whereas the emission 482 and 545 nm corresponds to $^5\text{D}_4$ to $^7\text{F}_j$ ($j = 6, 5$) transition of Tb^{3+} . The presence of emission peaks 365 and 379 was unexpected, also the transitions responsible to this emission are not known as it observed in further studies also. We have also measured the emission from 300 nm but no emission from Ce^{3+} was observed. This result shows that Ce^{3+} absorption in the $\text{Tb}^{3+}-\text{Ce}^{3+}$ system is much stronger than that of Tb^{3+} , because it is a spin and dipole allowed transition. Therefore the energy transfer from Ce^{3+} to Tb^{3+} or Ce^{3+} sensitization effect dominates the energy process. These facts indicate that energy transfer from Ce^{3+} to Tb^{3+} in the co-doped sample takes place. The enhanced intensity of the $^5\text{D}_3$ to $^7\text{F}_j$ transitions of Tb^{3+} in figure5.6 is very much possible because of the energy transfer process taken place in the region from 350 to 500nm [23]. The PL emission spectrum doesn't change much when measured for 240 nm excitation except in the reduction in the intensity. The ground state configuration of the Tb^{3+} ion is $4f^8$ and the excited state configuration is $4f^75d_1$, in which the $4f$ shell is half-filled. As the $4f$ shell is well shielded by the outer electrons within the $5s$ and $5p$ orbits, the $4f \rightarrow 4f$ transitions of Tb^{3+} are hardly influenced by the environments. Thus, Tb^{3+} shows $4f-4f$ sharp line emission. Additionally, the $4f5d$ excitation band is normally located at higher energies (< 254 nm), so in order to absorb the 254 nm radiation efficiently, the Ce^{3+} ion is used as a sensitizer through the energy transfer $\text{Ce}^{3+} \rightarrow \text{Tb}^{3+}$. For example in the case of the commercial phosphor $\text{CeMgAl}_{10}\text{O}_{19}:\text{Tb}^{3+}$ (CAT) for use in mercury gas-discharge lamps, by this way Tb^{3+} yields efficient green emission from the $^5\text{D}_4$ (to $^7\text{F}_j$, $j = 6 - 0$) level [24]. Ce^{3+} has been established as a luminescence sensitizer for the Tb^{3+} ion. The energy transfer process leading to the

enhancement of the Tb^{3+} $4f-4f$ transition originates from the metastable lowest $5d$ state of the Ce^{3+} ion, and under the proper conditions, the energy transfer rate can be high enough to change the emission dynamics of the donor state.

3.4 Thermoluminescence (TL) Characteristics of $\text{Sr}_3\text{Al}_2\text{O}_6:\text{Tb}^{3+}, \text{Eu}^{3+}$ Phosphor

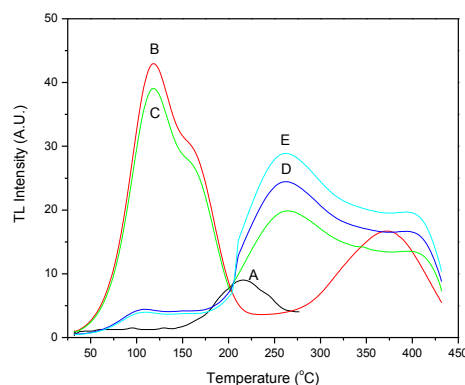


Fig. 5: Thermoluminescence glow curve of $\text{Sr}_3\text{Al}_2\text{O}_6:\text{Tb}^{3+}$ (1%), Eu^{3+} (x%) phosphor
Curve A = $\text{Sr}_3\text{Al}_2\text{O}_6:\text{Eu}^{3+}$ (1%); B = $\text{Sr}_3\text{Al}_2\text{O}_6:\text{Tb}^{3+}$ (1%);
C = $\text{Sr}_3\text{Al}_2\text{O}_6:\text{Tb}^{3+}$ (1%), Eu^{3+} (0.025%); D = $\text{Sr}_3\text{Al}_2\text{O}_6:$
 Tb^{3+} (1%), Eu^{3+} (0.1%); E = $\text{Sr}_3\text{Al}_2\text{O}_6:\text{Tb}^{3+}$ (1%), Eu^{3+} (0.5%).

The energy transfer phenomenon in the $\text{Sr}_3\text{Al}_2\text{O}_6:\text{Tb}^{3+}, \text{Eu}^{3+}$ phosphor can also be observed using the thermoluminescence characteristics. The phosphors were subjected to the thermally stimulated luminescence (TL) studies to ascertain the defects present in the synthesized compounds. Figure 5 shows the thermoluminescence glow curve of the $\text{Sr}_3\text{Al}_2\text{O}_6:\text{Tb}^{3+}, \text{Eu}^{3+}$ phosphor, where the concentration of Eu^{3+} gradually increases whereas the concentration of Tb^{3+} kept constant at 1%. The test dose of 100 Gy from a β source (Sr-90) of 50 mCi strength was given to all samples. Earlier we reported the dosimetric study of the $\text{Sr}_3\text{Al}_2\text{O}_6:\text{Tb}^{3+}$ phosphor [14]. For comparison the glow curves of $\text{Sr}_3\text{Al}_2\text{O}_6:\text{Eu}^{3+}$ (1%) is also shown in the figure. The curve A shows the single low intensity peak at around 215 °C, whereas the curve B shows peaks around 124, 164 and 340 °C. The addition of Eu^{3+} in $\text{Sr}_3\text{Al}_2\text{O}_6:\text{Tb}^{3+}$ (1%) changes the glow curve pattern completely. The thermoluminescence glow curve C shows the peaks around 124, 164 and 262 °C. The intensity of the 124 and 164 °C peaks also decreases by small amount. A new peak at 262 °C is observed on addition of Eu^{3+} . The well defined and prominent peak of 340 °C changes into the shoulder of the 262 °C peak. The 262 °C peak shows the formation of new traps due to incorporation of Eu^{3+} in $\text{Sr}_3\text{Al}_2\text{O}_6:\text{Tb}^{3+}$ phosphor. The glow curve D shows that the peak of 124 and 164 °C has been reduced remarkably and the TL intensity of the 262 °C peak increases with small intensity. Further increase in the Eu^{3+} concentration to 0.5% doesn't affect

much to the intensity of 124 and 164 °C peaks as it has already low intensity, but it helps to improve the intensity of the 262 °C peak. The increase in the Eu^{3+} concentration decreases the main TL dosimetric peak of Tb^{3+} i.e., 124 and 164 °C peak. This suggests that the after addition of Eu^{3+} in the $\text{Sr}_3\text{Al}_2\text{O}_6:\text{Tb}^{3+}$ phosphor the tendency of the charges getting trapped at 124 and 164 °C peaks reduces and they managed to get trapped and new trapping level which is further deep at 262 °C. The 262 °C is also not stable and reduces drastically within 48 hours. Also this peak consists of very complicated structure having more than 3-4 small glow curves which was tough to isolate for calculation of TL parameters of this system.

3.4 Thermoluminescence (TL) Characteristics of $\text{Sr}_3\text{Al}_2\text{O}_6:\text{Tb}^{3+}\text{Ce}^{3+}$ Phosphor

Figure 6 shows the thermoluminescence glow curve of $\text{Sr}_3\text{Al}_2\text{O}_6:\text{Tb}^{3+}(0.025\%), \text{Ce}^{3+}(0.1\%)$ denoted as 'a' in the curve, $\text{Sr}_3\text{Al}_2\text{O}_6:\text{Tb}^{3+}(0.025\%), \text{Ce}^{3+}(0.05\%)$ denoted as 'b' in the curve and $\text{Sr}_3\text{Al}_2\text{O}_6:\text{Tb}^{3+}(0.025\%)$ denoted as 'c' in the curve. The above three phosphors were irradiated by beta rays from ^{90}Sr beta source to a dose of 100 Gy. The TL glow curve was recorded from room temperature to 200 °C for a heating rate of 2 K/s. Above this temperature the kanthal was showing black body radiations, so the peaks beyond 200 °C is suppose to be not reliable. The curve 'c' shows the general order peaks around 124 °C and a hump around 170 °C, which can be isolated by using the T_{stop} - Method, as we have studied this glow curve in the last chapter. This peak was studied as dosimetric peak. The curve 'a' represents the TL glow curve after incorporation of the $\text{Ce}^{3+}(0.1\%)$ in the $\text{Sr}_3\text{Al}_2\text{O}_6:\text{Tb}^{3+}(0.025\%)$. The addition of Ce^{3+} in the system changes the concentration of the traps. The peak at 124 °C transforms into hump and the hump of the curve 'c' i.e. the peak of 170 °C, now in this case appears as a prominent peak. The intensity of the 170 °C peak increases drastically as shown in the figure, where it is reduced by a factor of 10 for comparison. The increase in the TL intensity of the dosimetric peak is the positive feature of the incorporation of Ce^{3+} as a co-dopant in the $\text{Sr}_3\text{Al}_2\text{O}_6:\text{Tb}^{3+}$ phosphor. Also the fluorescence emission of the $\text{Sr}_3\text{Al}_2\text{O}_6:\text{Tb}^{3+}(0.025\%), \text{Ce}^{3+}(0.1\%)$ shows the bluish green emission which has application as a bluish green lamp phosphor[18-33]. The TL intensity of the 170 °C peak of this phosphor reduces to 20% after 2 months of storage in the dark. This studies indicates that the phosphor $\text{Sr}_3\text{Al}_2\text{O}_6:\text{Tb}^{3+}(0.025\%), \text{Ce}^{3+}(0.1\%)$ can be used as lamp phosphor as well as dosimetric application.

The TL glow curve of $\text{Sr}_3\text{Al}_2\text{O}_6:\text{Tb}^{3+}(0.025\%), \text{Ce}^{3+}(0.05\%)$ is as shown as curve 'b' in the figure. The TL peaks are not defined in this glow curve. The trap is not well separated as well as defined. May be the reason behind such luminescence is the low concentration of the $\text{Ce}^{3+}(0.05\%)$ in the $\text{Sr}_3\text{Al}_2\text{O}_6:\text{Tb}^{3+}(0.025\%)$ phosphor. The lower concentration of the Ce^{3+} doesn't help in the formation of traps or may be the formation of trap process

is in the intermediate state. Thus the $\text{Sr}_3\text{Al}_2\text{O}_6:\text{Tb}^{3+}(0.025\%), \text{Ce}^{3+}(0.05\%)$ phosphor cannot be considered as TL / PL phosphor.

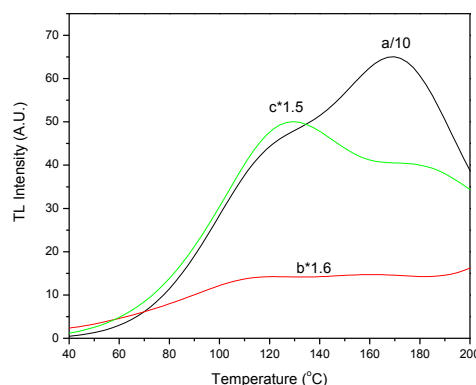


Fig. 6: TL glow curve of $\text{Sr}_3\text{Al}_2\text{O}_6: \text{Tb}, \text{Ce}$. Heating rate = 2 k/s Curve a = $\text{Sr}_3\text{Al}_2\text{O}_6: \text{Tb}(0.025\%), \text{Ce}(0.1\%)$; b= $\text{Sr}_3\text{Al}_2\text{O}_6: \text{Tb}(0.025\%), \text{Ce}(0.05\%)$; c = $\text{Sr}_3\text{Al}_2\text{O}_6: \text{Tb}(0.025\%)$.

4. CONCLUSION

From all the above results and discussion it can be conclude that the PL emissions of $\text{Sr}_3\text{Al}_2\text{O}_6:\text{Ce}^{3+}, \text{Tb}^{3+}$ phosphor shows emission in the bluish green region of the visible spectra and $\text{Sr}_3\text{Al}_2\text{O}_6:\text{Tb}^{3+}, \text{Eu}^{3+}$ shows emission as a yellowish light emitting lamp phosphor. The TL characteristics of this phosphor also show the energy transfer phenomenon in this phosphor.

ACKNOWLEDGEMENT

The authors are thankful to the Department of Atomic Energy, Government of India, for providing financial grant under the Board of Research in Nuclear Sciences (Grant No. 2002/37/18/BRNS).

REFERENCES

- [1] Y. Shimomura, N. Kijima, J. Electrochem. Soc. 151 (4), H86, 2004
- [2] W. Schaik, S. Lizzo, W. Smit, G. Blass, J. Electrochem. Soc. 140 (1), 216, 1993
- [3] R.S. Yadav, V.K. Shukla, L. Zheng, Jing Zhang, ECS J. Solid State Sci. Technol, 2 (4), R79, 2013.
- [4] D. Hou, W. Chen, X. Ding, H. Liang, Opt. Express 19, A1, 2011.
- [5] J. Liao, D. Zhou, H. You, H. Wen, Q. Zhou, B. Yang, Optik, 124, 1362, 2013.
- [6] C.H. Huang, T.W. Kuo, T.M. Chen, Opt P. Mishra, S.K. Pandey, K. Kumar, V. Baranwal, M. Kumar, A.C. Pandey, J. Alloys Compd., 547, 1, 2013.
- [7] T.W. Kuo, T.M. Chen, Opt. Mater., 32, 882, 2010.
- [8] D.L. Dexter, J. Chem. Phys. 21 (1953) 836.

- [9] G. Blasse. Luminescent Materials, Springer, Berlin (1994) 93.
- [10] T. Katsumata, R. Sakai, S. Komuro, T. Morikawa, J. Electrochem. Soc. 150, H111, 2003.
- [11] D. Wang, Y. Li, Y. Xiong, Q. Yin, J. Electrochem. Soc. 152, H12, 2005
- [12] P. Page, R. Ghildiyal, K.V.R. Murthy, Mater. Res. Bull., 41, 1854, 2006
- [13] P. Page, R. Ghildiyal, K.V.R. Murthy, Mater. Res. Bull., 43, 353, 2008
- [14] P. Page and K.V.R. Murthy, Phil. Mag. Lett., 90 (9), 653, 2010.
- [15] JCPDS-ICDD Card No. 24-1187.
- [16] Murthy, K.V.R., Rao, C.A., Suresh, K., Rao, N.V.P., Rao, B.S., Walter Ratna Kumar, B., Rajasekhar, B.N., Rao, B.N. Ceramic materials (phosphors) for display applications, (2011) Eurasian Chemico-Technological Journal, 13 (1-2), pp. 1-4.
- [17] Kulkarni, S., Nagabhushana, B.M., Nagabhushana, H., Murthy, K.V.R., Shivakumara, C., Damle, R. (2011) Transactions of the Indian Ceramic Society, 70 (3), pp. 163-166.
- [18] Tawde, D., Srinivas, M., Murthy, K.V.R. (2011) Physica Status Solidi (A) Applications and Materials Science, 208 (4), pp. 803-807.
- [19] Nagabhushana, H., Nagabhushana, B.M., Madesh Kumar, M., Chikkahanumantharayappa, Murthy, K.V.R., Shivakumara, C., Chakradhar, R.P.S. (2011) Spectrochimica Acta - Part A: Molecular and Biomolecular Spectroscopy, 78 (1), pp. 64-69.
- [20] Page, P., Murthy, K.V.R. (2010) Philosophical Magazine Letters, 90 (9), pp. 653-662.
- [21] Senthil, T.S., Muthukumarasamy, N., Agilan, S., Thambidurai, M., Murthy, K.V.R., Balasundaraprabhu, R.. (2009) Journal of Optoelectronics and Advanced Materials, 11 (6), pp. 831-833.
- [22] Parmar, M.C., Zhuang, W.D., Murthy, K.V.R., Huang, X.W., Hu, Y.S., Natarajan, V. (2009) Indian Journal of Engineering and Materials Sciences, 16 (3), pp. 185-187.
- [23] Sastry, M.D., Gaonkar, M., Mane, S., Athavale, S., Murthy, K.V.R., Desai, S., Bagla, H., Ramchandran, K.T. (2008) Diamond and Related Materials, 17 (7-10), pp. 1288-1291.
- [24] Page, P., Ghildiyal, R., Murthy, K.V.R. (2008) Materials Research Bulletin, 43 (2), pp. 353-360.
- [25] Ghildiyal, R., Page, P., Murthy, K.V.R. (2007) Journal of Luminescence, 124 (2), pp. 217-220.
- [26] Murthy, K.V.R., Rey, L., Belon, P. (2007) Journal of Luminescence, 122-123 (1-2), pp. 279-283.
- [27] Page, P., Ghildiyal, R., Murthy, K.V.R. Synthesis, (2006) Materials Research Bulletin, 41 (10), pp. 1854-1860.
- [28] Murthy, K.V.R., Pallavi, S.P., Rahul, G., Patel, Y.S., Sai Prasad, A.S., Elangovan, D. (2006) Radiation Protection Dosimetry, 119 (1-4), pp. 350-352.
- [29] Murthy, K.V.R., Pallavi, S.P., Ghildiyal, R., Parmar, M.C., Patel, Y.S., Ravi Kumar, V., Sai Prasad, A.S., Page, A.G. (2006) Radiation Protection Dosimetry, 120 (1-4), pp. 238-241.
- [30] Natarajan, V., Murthy, K.V.R., Jayanth Kumar, M.L. (2005) Solid State Communications, 134 (4), pp. 261-264.
- [31] Murthy, K.V.R., Patel, Y.S., Sai Prasad, A.S., Natarajan, V., Page, A.G. (2003) Radiation Measurements, 36 (1-6), pp. 483-485.
- [32] Chakrabarty, B.S., Murthy, K.V.R., Joshi, T.R. (2002) Turkish Journal of Physics, 26 (3), pp. 193-197.
- [33] Chakrabarty, B.S., Murthy, K.V.R., Josh, T.R. (1999) Indian Journal of Pure and Applied Physics, 37 (2), pp. 136-141.